Water Modulated Framework Flexibility in NH$_2$-MIL-125: Highlights from ^{13}C Nuclear Magnetic Resonance

Silvia Pizzanelli, Angelo Freni, Larisa G. Gordeeva, and Claudia Forte

QUERY SHEET

This page lists questions we have about your paper. The numbers displayed at left are hyperlinked to the location of the query in your paper.

The title and author names are listed on this sheet as they will be published, both on your paper and on the Table of Contents. Please review and ensure the information is correct and advise us if any changes need to be made. In addition, please review your paper as a whole for typographical and essential corrections.

Your PDF proof has been enabled so that you can comment on the proof directly using Adobe Acrobat. For further information on marking corrections using Acrobat, please visit http://journalauthors.tandf.co.uk/production/acrobat.asp; https://authorservices.taylorandfrancis.com/how-to-correct-proofs-with-adobe/

The CrossRef database (www.crossref.org/) has been used to validate the references.

AUTHOR QUERIES

Q1   Please provide the academic title (i.e.: "Professor," "Associate Professor," "Assistant Professor," etc.) for corresponding author.

Q2   Please provide the authors name.

Taylor & Francis
Taylor & Francis Group

Water Modulated Framework Flexibility in NH$_2$-MIL-125: Highlights from ^{13}C Nuclear Magnetic Resonance

Silvia Pizzanelli[a], Angelo Freni[a], Larisa G. Gordeeva[b,c], and Claudia Forte[a]

[a]Institute of the Chemistry of Organometallic Compounds, CNR-ICCOM, Pisa, Italy; [b]Boreskov Institute of Catalysis, Novosibirsk, Russia; [c]Novosibirsk State University, Novosibirsk, Russia

ABSTRACT

The influence of adsorbed water on the dynamics of the organic linker 1,4-benzenedicarboxylate (BDC) in the metal organic framework NH$_2$-MIL-125 was examined by applying ^{13}C Nuclear Magnetic Resonance (NMR) spectroscopy on samples loaded with different amounts of water. In particular, the analysis of (i) cross-polarization (CP) ^{13}C Magic Angle Spinning (MAS) NMR spectra in terms of chemical shift and line width of the carbon signals, (ii) variable contact time ^{13}C CP-MAS experiments, and (iii) longitudinal ^{13}C relaxation times indicated that, upon hydration, a dynamic process occurring on the microseconds timescale accelerates. This process could be identified with the rotation of the BDC benzene ring about its C$_2$ axis, with water competing with the carboxylic oxygen for hydrogen bonding with the aminic group. Other motions occurring at frequencies on the order of the ^{13}C Larmor frequency, i.e. 75 MHz, which contribute to the flexibility of the three-dimensional network, were detected, and identified with the twisting, libration and translation of the BDC linker.

Introduction

Metal − organic frameworks (MOFs) are a class of promising hybrid materials for various potential applications in the field of gas storage and separation [1, 2] and thermal energy conversion [3–6], among others. The adsorption performance of MOFs has been primarily investigated from a thermodynamic point of view. Kinetic aspects of adsorption have also been addressed, usually focusing on the diffusion behavior of guest molecules [7–18]. However, the study of the concomitant dynamic response of the host framework is comparatively less common and only recently has become a hot topic [19, 20]. Indeed, contrarily to more traditional porous materials, such as zeolites, silica, or activated carbons, MOFs are more flexible. This flexibility can lead to the so-called breathing effect, characterized by large unit cell changes, but can also be related to minor motions, as local rearrangements of the organic linkers within the hybrid framework, which may give rise to the phenomenon known as gate-opening [21]. Therefore, gaining an understanding of MOFs flexibility at a microscopic level may drive the design of materials with enhanced adsorption selectivity and improved working capacity.

In the case of the local rearrangements of the organic linkers, the dynamics has been investigated in empty MOFs by experimental methods sensitive to different time scales [22–24], but only a few studies focused on the change of the framework dynamics in the presence of adsorbed species [25–27].

The present work aims to elucidate the influence of water on the motional behavior of the NH$_2$ functionalized 1,4-benzenedicarboxylate (BDC) ligands in NH$_2$-MIL-125. This microporous MOF is composed of Ti$_8$O$_8$(OH)$_4$-(NH$_2$-BDC)$_6$ units, where a cyclic inorganic octamer is built from TiO$_5$(OH) octahedra and is connected to other 12 octamers through NH$_2$-BDC linkers [28]. The octamers are packed according to a face centered cubic symmetry, with the NH$_2$-BDC linking them and providing a porous 3D structure [29, 30].

This MOF has been found to exhibit promising properties in the field of adsorption heat transformation and storage [31–33] from the point of view of water capacity and, consequently, thermodynamic efficiency, low temperature regeneration, minor

Q1

Nomenclature

BDC	1,4-benzenedicarboxylate
CP	Cross-Polarization
DE	Direct Excitation
F	Factor considering the geometry of motion, dimensionless
$\hbar$	Planck's constant, J·s
IRMOF	Isoreticular Metal Organic Framework
M(t)	Signal intensity at contact time t in a variable contact time CP-MAS experiment, arbitrary units
M*	Constant proportional to the number of carbon atoms contributing to the signal in a variable contact time CP-MAS experiment, arbitrary units
MAS	Magic Angle Spinning
MIL	Material of Institute Lavoisier
MOF	Metal Organic Framework
NMR	Nuclear Magnetic Resonance
ppm	Parts per million
p/p_0	Partial pressure of water over the sample divided by the saturated vapor pressure of water
r	Distance between C and H nuclei, m
SEM	Scanning Electron Microscopy
t	Contact time during cross-polarization, s
T_{CH}	CP time constant, μs
T_1	Longitudinal relaxation time in the laboratory frame, s
$T_{1\rho H}$	^1H longitudinal relaxation time in the rotating frame, ms

Greek symbols

γ^1_H	gyromagnetic ratio of ^1H nucleus, rad·s^{-1}·T^{-1}
γ_{13C}	gyromagnetic ratio of ^{13}C nucleus, rad·s^{-1}·T^{-1}
δ	chemical shift, ppm
$\Delta\nu$	line width, ppm
θ	pore-filling factor
ν_1	intensity of the ^1H radiofrequency used for $^1H/^{13}C$ decoupling expressed as a nutation frequency, Hz
τ_c	correlation time of a motion, s
ω_1	intensity of the ^1H radiofrequency used for $^1H/^{13}C$ decoupling expressed as a nutation frequency, rad/s

sensitivity of adsorption capacity and porosity to adsorption cycles, and efficiency and specific power of the chilling cycle. It has also been found to exhibit encouraging properties in the field of gas separation [34, 35] and liquid phase separation of hydrocarbons [36, 37].

Here, solid state Nuclear Magnetic Resonance (NMR) was employed to investigate the mobility of the BDC ligand. This technique has proven to be one of the most powerful tools for investigating local scale structure and dynamics in MOFs [38]. In particular, to gain insight into the framework mobility in the presence of adsorbed species, ^2H NMR spectroscopy has been often used [26, 27], a method requiring deuteration of the sample. In this study, we observed naturally occurring ^{13}C nuclei and no deuteration was needed. The line width of the ligand ^{13}C signals, recorded using Cross Polarization (CP) with Magic Angle Spinning (MAS), was monitored as a function of the water content, exploring relatively slow motions on the microseconds timescale. The analysis of variable contact time CP experiments allowed information on the effect of water on the BDC mobility to be obtained through the determination of the CP transfer rate constant, T_{CH}, and of the ^1H longitudinal relaxation time in the rotating frame, $T_{1\rho H}$. Faster dynamic processes were highlighted from the determination of ^{13}C longitudinal relaxation times in the laboratory frame, T_1, as a function of loading.

The combination of different ^{13}C solid state NMR methods allowed us to address the important issue of framework flexibility in a MOF characterized by promising properties in a variety of applications, for which an understanding the flexibility at a microscopic level is especially appealing.
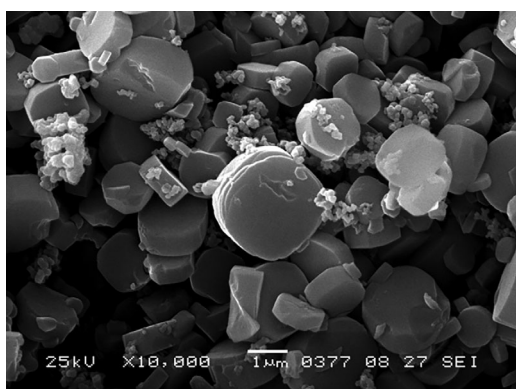
Experimental

NH$_2$-MIL-125 was synthesized according to the procedure described in Ref. [32]. The as-synthesized product was constituted by primary particles, with an average size of about 1.8 μm as determined by means of a scanning electron microscope JEOL JSM-6460. A scanning electron microscopy (SEM) image of NH$_2$-MIL-125 is shown in Figure 1.

The as-synthesized particles were dried at 150 °C in vacuo for 20 hours and then exposed to a humid atmosphere to progressively hydrate the sample. The hydration level was measured gravimetrically and is reported in terms of pore-filling factor, θ, i.e. the amount of adsorbed water divided by the maximum adsorbable amount, 0.45 g/g, as determined from the water adsorption isotherm at 21 °C at $p/p_0 = 0.43$ presented in Figure 2. Samples with θ ranging from 0 to 1 were prepared. The water adsorption isotherm was volumetrically measured, and the pore-filling factors of the samples investigated are reported in Figure 2.
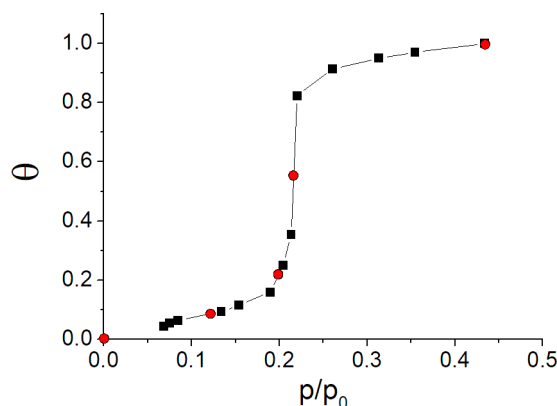
A selection of relevant thermophysical properties available from the literature for this material [32, 39] is given in Table 1.

Solid state ^{13}C NMR experiments were performed on a Bruker Avance Neo-300 WB spectrometer equipped with a 4 mm probe. The operating

Figure 1. SEM image of NH$_2$-MIL-125 revealing primary particles.

Figure 2. Water adsorption isotherm of NH$_2$-MIL-125 at 21 °C. The line joining the experimental points, represented by squares, was drawn to guide the eyes. The circles represent the filling factors of the samples examined in the present study.

Table 1. Selection of relevant thermophysical properties of NH$_2$-MIL-125 available from the literature.

Property	Value	Reference
Specific heat (J g^{-1} K^{-1})	0.8–1.2 in the range 300–375 K	[32]
Apparent density (g cm^3)	0.55	[39]
Isosteric enthalpy of water adsorption (kJ mol^{-1})	−54.9–−49.7 depending on loading	[32]

frequencies were 300.13 and 75.47 MHz for ^{1}H and ^{13}C, respectively. The ^{1}H and ^{13}C 90° pulse was 4.5 μs. The variable contact time ^{13}C CP-MAS experiments were carried out with contact time values ranging from 150 μs to 30 ms with a 75 kHz ^{1}H rf field. The CP spectra were acquired accumulating 7200 transients and the recycle delay was 3 s. The number of transients in the ^{13}C Direct Excitation (DE) spectra ranged between 500 and 1000 and the recycle delay was 125 s. The ^{13}C T$_1$ values were measured applying the Torchia sequence [40], with a contact time of 2 ms and a recycle delay of 3 s. At least 15 delays were used and 750 transients were acquired for each delay. The ^{1}H decoupling during signal acquisition was performed using the time proportional phase modulation scheme with a rf irradiation frequency, ν_1, of 62.5 kHz. The rotor spinning rate was 12 kHz. The chemical shifts were externally referenced to the upfield resonance of adamantane at 29.50 ppm. The deconvolution of the spectra was performed using the softwares dmfit [41] and SPORT-NMR [42]. The spectral peaks were fitted through mixed Gaussian/Lorentzian functions, with the line width defined as the full width at half maximum of the fitting function. The peak integrals determined from the deconvoluted spectra were used for the analysis of the variable contact time and Torchia experiments. The signal decays in the ^{13}C T$_1$ experiments were described by an exponential function, while the evolution of the signals in the variable contact time CP-MAS experiments was fitted using the following simplified expression [43]:

$$M(t) = M^* \left(1 - \frac{T_{CH}}{T_{1\rho H}} \right)^{-1} \left(e^{-\frac{t}{T_{1\rho H}}} - e^{-\frac{t}{T_{CH}}} \right) \qquad (1)$$

where M(t) represents the signal intensity at contact time t, M* is a constant proportional to the number of carbon atoms contributing to the signal, T$_{CH}$ represents the CP time constant, and T$_{1\rho H}$ the proton spin-lattice relaxation time in the rotating frame. When this fitting curve failed in reproducing the data, the following expression was used:

$$M(t) = M^* \left[\left(1 - \frac{T_{CH}}{T_{1\rho H1}} \right)^{-1} \left(e^{-\frac{t}{T_{1\rho H1}}} - e^{-\frac{t}{T_{CH}}} \right) \right.$$
$$\left. + \left(1 - \frac{T_{CH}}{T_{1\rho H2}} \right)^{-1} \left(e^{-\frac{t}{T_{1\rho H2}}} - e^{-\frac{t}{T_{CH}}} \right) \right] \qquad (2)$$

where two different relaxation times, T$_{1\rho H1}$ and T$_{1\rho H2}$, were required.

The fitting of the ^{13}C T$_1$ and variable contact time data were performed within the Mathematica 10 programming environment [44].

Results and discussion

The ^{13}C CP-MAS spectra of NH$_2$-MIL-125 at different water loading levels, recorded with a 2 ms contact time, are shown in Figure 3. The spectra highlighted the occurrence of structural and/or dynamic changes upon hydration which variably affected the line width and the chemical shift of the different signals. These were assigned to the carbon atoms as labeled in the
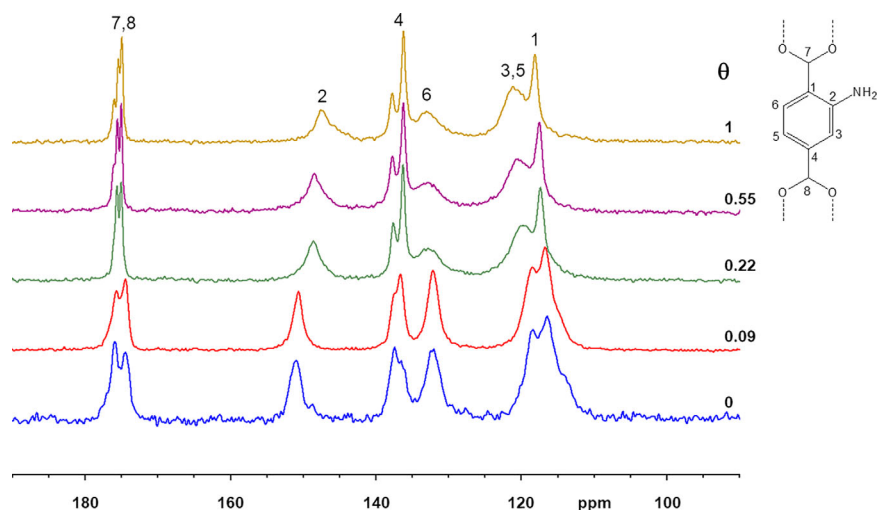
Figure 3. ^{13}C CP-MAS spectra of NH$_2$-MIL-125 at different pore-filling factors θ. The ^{13}C signals were assigned to the carbon atoms labeled in the chemical structure.
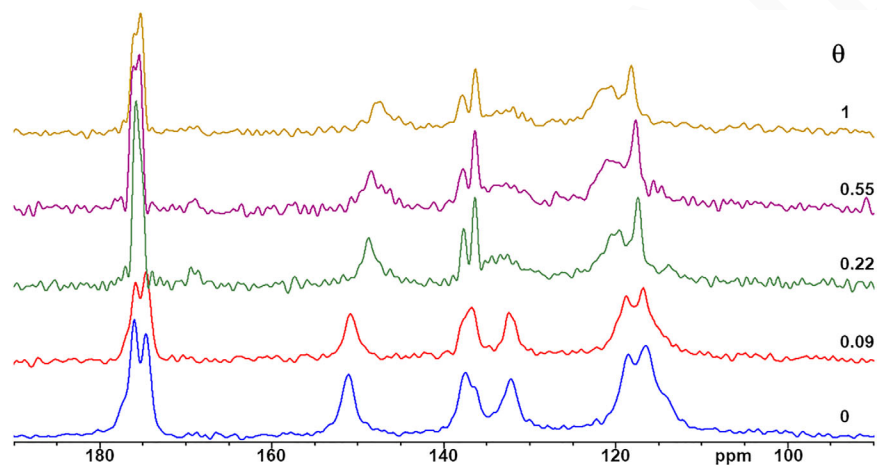
Figure 4. ^{13}C DE MAS spectra of NH$_2$-MIL-125 at the indicated pore-filling factors.

figure. The assignment was based on that reported in the literature [45]. No major differences were detected between CP and DE spectra (shown in Figure 4) apart from a significant decrease of the C-7, C-8 signals in the CP spectra compared to the other signals, due to the much lower efficiency of cross polarization for these carbons, which is expected considering the longer distance from the closest protons.

A first striking feature, more evident in the more hydrated samples, is the presence of more signals than the eight expected, considering the inequivalent carbon nuclei of each NH$_2$ substituted BDC unit, and differently from IRMOF-3, a Zn MOF with the same ligand, reported in the literature [45]. In particular, the C-4 signal clearly showed a doublet with 2:1 relative intensity, at least for pore-filling factors $\theta \geq 0.09$. A similar doublet was also observable for one of the carboxylate C signals. These doublets were tentatively attributed to slight structural differences in the

carboxylate linkage to the Ti atoms for the ligands linking two octamers on the same plane and those linking two octamers on different planes [30], the number of the former type of ligands being half of those of the latter type.

Furthermore, the spectra show changes in the position of the signals upon water loading, the chemical shift also depending on the water loading level. The chemical shift values for each signal and for the different samples are reported in Table 2. The variation in chemical shift provides insights into the homogeneity of water distribution in the matrix and on the most hydrophylic centers. In particular, the chemical shifts gradually changed, with no contribution from the dry sample persisting at the higher hydration degrees. This indicates that water was homogeneously distributed in all the crystallites. The chemical shift of the C-2 carbon atom, which is bound to the amino group, was the most sensitive to filling level, with an upfield

Table 2. Chemical shifts, δ (ppm) and line widths (ppm) of the carbon signals in the BDC unit of NH$_2$-MIL-125 at different pore-filling factors θ.[a]

θ	0		0.09		0.22		0.55		1.00	
Carbon	δ	Line width	δ	Line width	δ	Line width	δ	Line width	δ	Line width
C-1	116.38	3.3	116.65	2.4	117.33	1.2	117.58	1.1	118.15	1.1
C-2	151.03	1.6	150.73	1.4	148.62	2.5	148.48	2.5	147.30	2.5
C-3, C-5	118.63	1.6	118.77	1.9	119.87	3.7	120.44	3.6	120.98	3.6
C-4 1	136.36	1.2	136.60	1.1	136.27	0.8	136.27	0.8	136.23	0.8
C-4 2	137.54	1.2	137.57	0.9	137.61	0.7	137.78	0.7	137.80	0.7
C-6	132.17	2.1	132.14	1.6	132.76	3.7	132.93	3.8	132.88	3.7
C-7, C-8 1	175.95	1.2	175.77	1.2	176.08	0.5	176.16	0.5	176.06	0.5
C-7, C-8 2	174.74	0.8	174.77	1.2	175.63	0.5	175.60	0.4	175.45	0.4
C-7, C-8 3	174.22	0.8	174.32	0.8	175.02	0.5	175.05	0.4	174.97	0.4

[a]The ^{13}C chemical shifts and the line widths were determined by fitting the signals in the CP spectra.

shift of more than 3 ppm upon complete hydration, whereas C-1, C-3 and C-5 experienced a 2 ppm downfield shift. These trends can be interpreted considering that water competes with the carboxylic oxygen for hydrogen bonding with the aminic group. Consequently, the nitrogen lone-pair is less available for conjugation with the aromatic ring and hence reduces electron density in the ortho and para positions (C-1, C-3 and C-5) according to a mesomeric effect, causing a downfield shift of the corresponding signals. On the other hand, the opposite trend of the C-2 signal is determined by an inductive effect. For the remaining signals the shift was negligible. In addition, the changes of the mentioned chemical shifts were more pronounced at low loadings and tended to level off upon increasing the hydration level. This indicates that at low fillings water molecules preferentially bind to the hydrophylic NH$_2$ groups and thus significantly perturb their magnetic environment. Additional water molecules induce a smaller perturbation on the amino environment because they are located farther from the NH$_2$ groups in comparison with the pre-adsorbed water molecules, with which they probably form hydrogen bonds. This pore filling mechanism was suggested to explain the S-shaped isotherms of this material [32].

The CP-MAS spectra also showed relevant changes in line widths for θ passing from 0.09 to 0.22, remaining constant for higher filling levels. The ^{13}C line width of the CP-MAS peaks provides information on relatively slow molecular motions, i.e. on timescales on the order of 10^{-7}–10^{-5} s. The signals due to C-2, C-3, C-5, and C-6 experienced a sudden broadening at $\theta = 0.22$, whereas the C-1, C-4, C-7, and C-8 signals tended to sharpen up to $\theta = 0.22$. The line widths determined from the spectral deconvolution are reported in Table 2.

In general, signal broadening could arise from the interference between a molecular motion and the ^{1}H decoupling. In fact, a molecular motion modulating

the dipolar interaction with a frequency on the order of that of the ^{1}H decoupling field, ω_1, is expected to give a contribution to the ^{13}C line width, $\Delta\nu$, given by the following expression [46]:

$$\Delta\nu \cong (1-F)\frac{1}{\pi}\frac{\gamma_{^1H}^2\gamma_{^{13}C}^2\hbar^2}{r^6}\left(\frac{\tau_c}{1+\omega_1^2\tau_c^2}\right) \quad (3)$$

where τ_c is the correlation time of the motion, r is the distance between C and H nuclei, $\gamma_{^1H}$ and $\gamma_{^{13}C}$ are the gyromagnetic ratios of ^{1}H and ^{13}C nuclei, respectively, and $\hbar$ is Planck's constant. F is a factor that considers the geometry of the motion. Three different regimes may apply: (i) $\omega_1\tau_c \ll 1$, implying that $\Delta\nu \propto \tau_c$ and that the line broadening is independent of the rf decoupling and typically the line is motionally narrowed; (ii) $\omega_1\tau_c \cong 1$ and in this case the line is broadest; (iii) $\omega_1\tau_c \gg 1$, which means that $\Delta\nu \propto \left(\frac{1}{\omega_1^2\tau_c}\right)$ and the broadening depends on the rf decoupling strength. Considering that in our experiments $\omega_1 = 2\pi\,\nu_1 = 2\pi\,62.5$ kHz, broadening indicates the presence of a motion in the microseconds timescale, a maximum being expected at $\tau_c \cong 2.5$ μs. A plausible motion on this timescale could be the π flip of the aromatic ring around the two-fold axis, considering that comparable correlation time values were found for BDC ring rotational dynamics in other MOFs [22–26]. In a previous study on dry NH$_2$-MIL-125, a lower boundary of 2.2 μs was determined for the rotational correlation time of the N-H bond [47]. Since the N-H bond is anchored to an aromatic carbon and can move together with the ring and/or move independently through rotation around the C-N bond, its motion will be characterized by a correlation time equal to or shorter than that of the aromatic ring. Hence, the lower boundary limit of 2.2 μs applies also to the π flip. This limiting value is very close to the τ_c value corresponding to the maximum line width, indicating that, for the dry MOF, the aromatic flip is in the slow-motion regime (iii). The significant broadening of the

C-3, C-5, and C-6 signals at $\theta = 0.22$ is therefore an indication of an acceleration of the π flip motion. The insignificant further variation of the line widths of the C-3, C-5, and C-6 signals at loadings above 0.22 indicates that this motion is not substantially accelerated with higher water content.

No analogous broadening was observed for the C-1, C-4, C-7, and C-8 signals. This can be explained considering the longer distance between these carbons and the closest protons, and hence the smaller dipolar decoupling interference effect. On the contrary, these signals sharpened upon hydration, reaching almost half their initial line width at $\theta = 0.22$ and remaining constant above this value. This effect can be ascribed to the presence of a high frequency motion which, upon hydration, would give a more efficient averaging of the interactions contributing to the line width not completely averaged by MAS, such as chemical shift anisotropy. As far as the C-2 signal broadening is concerned, it should be pointed out that this signal is significantly affected by the presence of the quadrupolar ^{14}N nucleus bound to it [48].

Variable contact time ^{13}C CP-MAS experiments were performed to gain further insight into the dynamics of the system. In fact, the evolution of the magnetization, M(t), during the contact time, t, described in Eq. (1), is governed by the proton spin-lattice relaxation time in the rotating frame, $T_{1\rho H}$, and the cross polarization time constant, T_{CH}, which are related to the dynamics of the system. $T_{1\rho H}$ is sensitive to the strength of the static ^1H-^1H dipolar interaction experienced by a hydrogen atom in close proximity to the detected carbon and to its dynamics in the frequency range 10^4–10^5 kHz. If the motional

frequency is smaller than the strength of the ^1H rf irradiation field in frequency units, here equal to 75 kHz, an acceleration of the motion will cause a decrease in $T_{1\rho H}$, eventually reaching a minimum value when the frequency becomes equal to that of the rf field and then increasing for further acceleration. It is worth to point out that for protons in short-range spatial proximity (in the nanometer length scale) spin diffusion may occur whereby the $T_{1\rho H}$ values for protons with different intrinsic relaxation rates are averaged. As far as T_{CH} is concerned, its value gives an indication of the strength of the ^1H-^{13}C dipolar interaction, which depends on the ^1H-^{13}C internuclear distance and on the motion of the ^1H-^{13}C internuclear vector, as well as on the number of protons close to the carbon. The stronger the interaction, the more rigid is the system and the higher the number of protons involved in the CP process, the shorter the value of T_{CH}.

The experimental build-up curves of selected carbon signals as a function of contact time for NH$_2$-MIL-125 loaded at $\theta = 0.09$ and 1 are shown in Figure 5 together with the corresponding fitting curves obtained using Eq. (1), whereas the parameters T_{CH} and $T_{1\rho H}$ are reported in Table 3 for each carbon.

In agreement with what expected based on the ^{13}C-^1H distances, the protonated carbons showed the shortest T_{CH} values, whereas the carboxylate carbons exhibited the longest ones. Upon increasing the hydration level, the C-3, C-5, C-6 T_{CH} values tended to moderately increase, suggesting a slight decrease in the dipolar interaction ascribable to an increased mobility of the ring, with motional timescales on the order of 10 µs or shorter, as for example the π flip
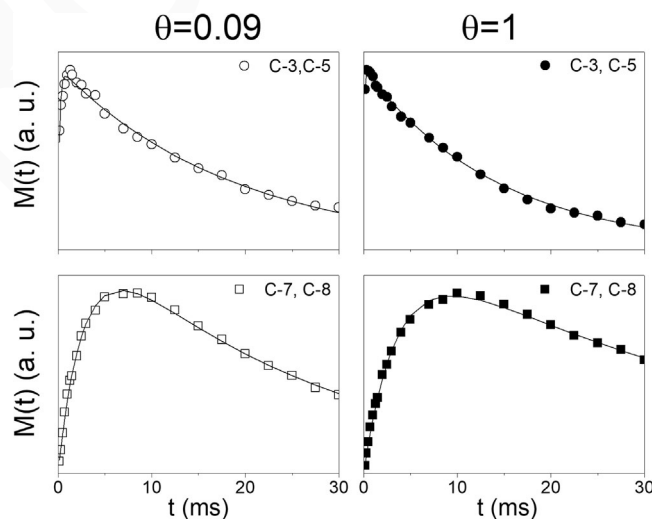
Figure 5. Experimental build-up curves of the carbon signals, C-3, C-5 and C-7, C-8, as a function of contact time, t, obtained by applying variable contact time ^{13}C CP-MAS experiments on NH$_2$-MIL-125 loaded at $\theta = 0.09$ (left-hand-side) and 1 (right-hand-side). Continuous lines are obtained from fitting of the curves according to Eq. (1).

discussed above. However, contributions from other motions cannot be excluded. As a matter of fact, different techniques have shown that, in some MOFs, the aromatic ring of the BDC linker is subject to the motions sketched in Figure 6, consisting in librations, out of phase transverse motion and translation and that the carboxylate groups experience local twisting and vibrational motion [22, 49, 50]. The same motions would be the cause of the dramatic increase in the T_{CH} values of the non protonated C-1, C-4, C-7, C-8 carbons; in this case, besides affecting the orientation of the C-H internuclear vector, some of the motions depicted in Figure 6 also modulate the ^1H-^{13}C distance. The carbon bonded to the amino group showed a peculiar behavior. In the less hydrated sample a T_{CH} value significantly shorter than that displayed by C-1, which has an aromatic proton at approximately the same distance, could be ascribed to cross-polarization also from the closer aminic protons. On the other hand, at the highest hydration level the C-2 T_{CH} was close to the values observed for the non protonated aromatic carbons, indicating that the cross-polarization from the aminic

protons is no more effective, probably because of water exchange and aminic group rotation.

Concerning the $T_{1\rho H}$ values, no significant differences among the carbon atoms of the less hydrated MOF were detected, the values being clustered around 20–24 ms, with the exception of C-2, for which a shorter value of 11 ms was observed, indicating the inefficiency of spin diffusion in averaging the different $T_{1\rho H}$ values. This may be quite surprising considering the rigidity of the system and the proximity of the protons for each BDC unit; however, this phenomenon has been demonstrated to occur for local spin diffusion processes where dipolar couplings with other nuclei (here ^{13}C and ^{14}N) may quench the flip-flop magnetization transfer between neighboring protons [51]. As a matter of fact, the fitting of the C-2 build-up curve could be significantly improved considering a bi-exponential decay, ascribable to cross-polarization of the C-2 carbon from two different types of protons, i.e. the aminic protons and the aromatic H-3 proton in the ortho position, as shown in Figure 7. It is worth to point out that the longer $T_{1\rho H}$ value, 19 ± 3 ms, is, within experimental error, in the range of values detected from the other aromatic carbons, and hence ascribable to the aromatic protons.

The insignificant differences among the $T_{1\rho H}$ values obtained from the other carbon atoms are not surprising since these values are relative to aromatic protons which experience comparable static homonuclear dipolar interaction and mobility.

Upon hydration, the $T_{1\rho H}$ values measured for C-2, C-7 and C-8 significantly increased, whereas the C-3, C-5 and C-6 $T_{1\rho H}$ ones tended to decrease and the C-1 and C-4 ones increased only slightly. All this indicates the presence of different proton pools giving cross-polarization to the different types of carbons. The lengthening of the C-2 $T_{1\rho H}$ can be explained considering that the aminic protons do not participate

Table 3. CP time constant, T_{CH}, and ^1H spin-lattice relaxation time in the rotating frame, $T_{1\rho H}$, of the carbon signals in the BDC unit of NH$_2$-MIL-125 at selected pore-filling factors θ.[a]

| θ | 0.09 | | 1.00 | |
Carbon	T_{CH} (μs)	$T_{1\rho H}$ (ms)	T_{CH} (μs)	$T_{1\rho H}$ (ms)
C-1	1400 ± 200	24 ± 3	2200 ± 200	27 ± 3
C-2	530 ± 50	11 ± 2	1500 ± 200	22 ± 3
C-3, C-5	100 ± 10	20 ± 3	120 ± 10	15 ± 3
C-4 1	1100 ± 200	21 ± 3	1300 ± 200	25 ± 3
C-6	100 ± 10	24 ± 3	160 ± 20	15 ± 3
C-7, C-8	2700 ± 200	24 ± 3	3700 ± 300	40 ± 3

[a]For the partially overlapped C-1 and C-3, C-5 signals, the parameters were obtained separately for C-1 and C-3, C-5 carbon atoms after deconvolution of the signal in the region at about 115–120 ppm into two distinct peaks. For C-7 and C-8, no deconvolution was performed, and the parameters were obtained considering the integral of the region including the signals.
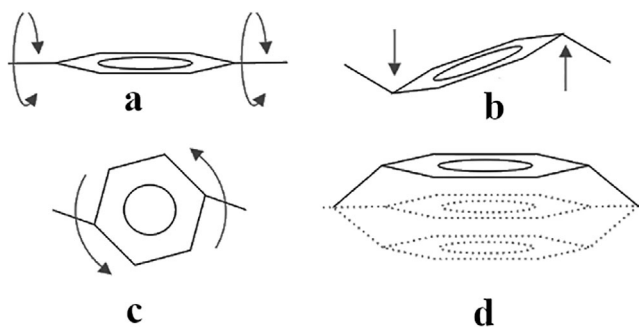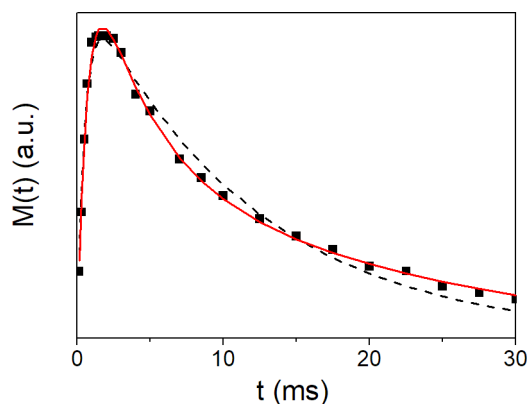

Figure 6. Sketches of possible simple motions of the benzene ring: libration around the para-axis (a), out-of-phase transverse motion (b), libration around an axis perpendicular to the benzene plane (c), in-phase transverse motion (d). Adapted with permission from reference [46]. Copyright 2010 American Chemical Society.

in the cross-polarization process because they exchange with water. The increase in the $T_{1\rho H}$ for the other non protonated carbons can be explained assuming the contribution of protons belonging to nearby relatively immobile water molecules, probably hydrogen-bonded to the carboxylic oxygens. This would represent the major contribution for the C-7 and C-8 carbons, whereas, in the case of the C-1 and C-4 ones, the contribution from the closer aromatic protons would be more significant, mitigating the effect of water on the $T_{1\rho H}$ value. The slight decrease of the C-3, C-5 and C-6 $T_{1\rho H}$ values is ascribable to an acceleration in the dynamics of the aromatic ring, revealing a motion with a correlation time in the microseconds timescale, in agreement with the findings from the changes in line widths.

To obtain information on the faster dynamic processes invoked in the discussion on the T_{CH} values, we measured the ^{13}C longitudinal relaxation times in the laboratory frame, T_1, as a function of loading. This relaxation time is sensitive to motions occurring at frequencies comparable to the ^{13}C Larmor frequency, here 75 MHz. The measured values are reported in Table 4. In the dry MOF, all the carbon atoms were characterized by T_1 values in the range 5–9 s. These values did not significantly change upon hydration up to $\theta = 0.09$, but suddenly increased at $\theta = 0.22$, further increasing for $\theta = 0.55$ and then remaining constant. The increase was more pronounced for the non protonated carbons C-1, C-4, C-7 and C-8. The observed ^{13}C T_1 values were surprisingly short, considering that typical values measured for diamagnetic crystalline materials range from tens to hundreds of seconds [52, 53]. The low T_1 values are a clear indication of the occurrence of substantial fast molecular motions. These can be identified with the twisting and libration of the BDC linker, as sketched in Figure 6. Although the dynamic processes are common to all the aromatic carbons, their effect on T_1 is different because the interactions involved are different. In particular, for the protonated aromatic carbons C-3, C-5 and C-6 the dominant interaction is the ^1H-^{13}C dipolar coupling involving the directly bonded proton, whereas ^{13}C chemical shift anisotropy gives a strong contribution to the relaxation of the non protonated aromatic carbons C-1 and C-4. The aromatic carbon bonded to the aminic group may be also influenced by the dipolar coupling to the ^{14}N nucleus. Furthermore, in the case of the C-1 and C-4 carbons, a contribution from the intermolecular dipolar interaction with water protons bonded to the carboxylate oxygens cannot be excluded. The slight difference in the T_1 values shown by carbons C-7 and C-8 compared to the non protonated aromatic carbons is to be ascribed to the different dipolar and chemical shift anisotropy interactions experienced by the two carbon sets. In addition, the comparison of T_1 and line width dependences on loading suggests some sort of correlation between the acceleration of the fast dynamic processes and of the relatively slow π flip, implying that, once water binds to the aminic group and hence renders the aromatic ring flip energetically less demanding, the fast processes are also speeded up.

Figure 7. C-2 cross-polarization signal as a function of contact time, t, in the variable contact time CP experiment and fitting curves obtained assuming a mono- (dashed curve, $T_{1\rho H}$ equal to 11 ± 2 ms, Eq. (1)) and a bi-exponential decay (solid curve, $T_{1\rho H1}$ and $T_{1\rho H2}$ equal to 19 ± 3 and 3.0 ± 0.5 ms, Eq. (2)) for the sample characterized by the pore-filling factor $\theta = 0.09$.

Table 4. ^{13}C longitudinal relaxation time, T_1 (s), of the carbon signals in the BDC unit of NH$_2$-MIL-125 at different pore-filling factors θ.[a]

Carbon	$\theta = 0$	$\theta = 0.09$	$\theta = 0.22$	$\theta = 0.55$	$\theta = 1.00$
C-1	6.8 ± 0.6	12.1 ± 0.8	20 ± 1	19.3 ± 0.7	19.3 ± 0.7
C-2	5.4 ± 0.5	8.6 ± 0.8	9.2 ± 0.8	9.0 ± 0.7	9.0 ± 0.7
C-3, C-5	5.2 ± 0.4	8.4 ± 0.6	10.3 ± 0.5	9.3 ± 0.8	9.3 ± 0.8
C-4	7.1 ± 0.6	14.8 ± 0.7	19 ± 1	18.2 ± 0.8	18.2 ± 0.8
C-6	5.6 ± 0.5	7.8 ± 0.6	9.4 ± 0.8	10.0 ± 0.8	10.0 ± 0.8
C-7, C-8	8.7 ± 0.5	16 ± 1	25 ± 1	25 ± 1	25 ± 1

[a]For the partially overlapped C-1 and C-3, C-5 signals, the parameters were obtained separately for C-1 and C-3, C-5 carbon atoms after deconvolution of the signal in the region at about 115-120 ppm into two distinct peaks. For C-7 and C-8, no deconvolution was performed, and the parameters were obtained considering the integral of the region including the signals.

Conclusions

By means of solid state ^{13}C NMR we have demonstrated that the flexibility of NH_2-MIL-125 framework is modulated by water and provided a picture of the role of water at a microscopic level. In particular, a motion involving the BDC ligands, occurring on the microseconds timescale and identified with π flips of the benzene rings about the two-fold axis, is accelerated when the pore-filling factor reaches the threshold value of 0.22. Additional water does not influence this motion. Simultaneously, fast dynamic processes, probably involving twisting, libration and translation of the BDC linker, are accelerated.

This study contributes to provide an understanding of the mechanisms according to which a guest molecule, in this case water, affects the linker mobility in a MOF, which is fundamental for envisaging possible applications.

Additional ^{13}C measurements at different temperatures and rf decoupling fields together with the determination of transverse relaxation times for isolating the contribution of the rf decoupling/motion interference to the line width could provide a more detailed picture of the role played by water in modulating NH_2-MIL-125 flexibility.

Acknowledgments

Notes on contributors

Silvia Pizzanelli is a researcher at the Institute of the Chemistry of Organometallic Compounds of the Italian National Research Council. She received her Ph.D. in Chemistry from the University of Pisa in 2001 and was a post-doc at Weizmann Institute of Science in Israel in 2003. Her research is focused on the application of solution and solid state NMR to small molecules and materials. She coauthored 31 papers on international scientific journals, 1 book on chemical physics (edited by ETS Pisa), 38 contributions to conferences.

Angelo Freni is a senior researcher at the Italian National Council of Research-Institute for the Chemistry of OrganoMetallic Compounds (CNR–ICCOM)–Pisa, Italy. He holds a Ph.D. in Materials and Chemical engineering from the University of Messina. His scientific interest concerns the field of energy technologies with special regard to thermally-driven heat pumps, heat storage and hydrogen storage systems. He has coauthored more than 180 papers on international Journals and conference proceedings.

Larisa G. Gordeeva is a leading researcher at the Boreskov Institute of Catalysis (BIC) SB RAS Novosibirsk, Russia. She received her Ph.D. in Chemical Kinetics and Catalysis at BIC in 1998, and Dr. Sci. degree (Dr. Hab.) in Physical Chemistry at the same Institute in 2013. Her research is focused on the material chemistry, adsorption, nanocomposites salt/matrix, MOFs, adsorption heat transformation and storage. She coauthored about 90 papers on international scientific journals, 1 book, and 70 communications at conferences.

Claudia Forte is a senior researcher at the Institute of the Chemistry of Organometallic Compounds of the Italian National Research Council. She received her Ph.D. in Chemistry from the University of Pisa in 1987. She studied at the University of Pisa and at the Scuola Normale Superiore in Pisa where she obtained her MS degree in chemistry in 1982. Her research activity is focused on the application of solution and solid state NMR techniques for the investigation of the structural and dynamic properties of complex materials of interest for biomedical, environmental and technological applications. She is coauthor of more than 110 publications on international peer-reviewed journals and over 200 contributions to international conferences.

References

[1] R.-B. Lin, S. Xiang, H. Xing, W. Zhou, and B. Chen, "Exploration of porous metal–organic frameworks for gas separation and purification," *Coord. Chem. Rev.*, vol. 378, pp. 87–103, Jan. 2019. DOI: 10.1016/j.ccr.2017.09.027.

[2] H. Li, et al., "Recent advances in gas storage and separation using metal–organic frameworks," *Mater. Today*, vol. 21, no. 2, pp. 108–121, Mar. 2018. DOI: 10.1016/j.mattod.2017.07.006.

[3] M. F. de Lange, K. J. F. M. Verouden, T. J. H. Vlugt, J. Gascon, and F. Kapteijn, "Adsorption-driven heat pumps: the potential of metal-organic frameworks," *Chem. Rev.*, vol. 115, no. 22, pp. 12205–12250, Nov. 2015. DOI: 10.1021/acs.chemrev.5b00059.

[4] S. K. Henninger, F. Jeremias, H. Kummer, and C. Janiak, "MOFs for use in adsorption heat pump processes," *Eur. J. Inorg. Chem.*, vol. 2012, no. 16, pp. 2625–2634, Jun. 2012. DOI: 10.1002/ejic.201101056.

[5] S. Cui, et al., "Metal-organic frameworks as advanced moisture sorbents for energy-efficient high

953 954 temperature cooling," *Sci. Rep.*, vol. 8, no. 1, p. 15284, Oct. 2018. DOI: 10.1038/s41598-018-33704-4.

955 956 957 958 959 [6] J. J. Jenks, R. K. Motkuri, W. TeGrotenhuis, B. K. Paul, and B. P. McGrail, "Simulation and experimental study of metal organic frameworks used in adsorption cooling," *Heat Transf. Eng.*, vol. 38, no. 14–15, pp. 1305–1315, 2017. DOI: 10.1080/01457632.2016.1242965.

960 961 962 963 964 965 [7] V. Bon, et al., "Characteristics of flexibility in metal-organic framework solid solutions of composition [Zn$_2$(BME-bdc)x(DB-bdc)2-xdabco]n: in situ powder X-ray diffraction, in situ NMR spectroscopy, and molecular dynamics simulations," *Micropor. Mesopor. Mater.*, vol. 216, pp. 64–74, Nov. 2015. DOI: 10.1016/j.micromeso.2015.02.042.

966 967 968 969 970 [8] V. J. Witherspoon, J. Xu, and J. A. Reimer, "Solid-state NMR investigations of carbon dioxide gas in metal-organic frameworks: insights into molecular motion and adsorptive behavior," *Chem. Rev.*, vol. 118, no. 20, pp. 10033–10048, Oct. 2018. DOI: 10.1021/acs.chemrev.7b00695.

971 972 973 [9] J.-R. Li, R. J. Kuppler, and H.-C. Zhou, "Selective gas adsorption and separation in metal-organic frameworks," *Chem. Soc. Rev.*, vol. 38, no. 5, pp. 1477–1504, May 2009. DOI: 10.1039/B802426J.

974 975 976 977 978 [10] E. M. Forman, B. R. Pimentel, K. J. Ziegler, R. P. Lively, and S. Vasenkov, "Microscopic diffusion of pure and mixed methane and carbon dioxide in ZIF-11 by high field diffusion NMR," *Micropor. Mesopor. Mater.*, vol. 248, pp. 158–163, Aug. 2017. DOI: 10.1016/j.micromeso.2017.04.041.

979 980 981 982 [11] S. Schlayer, et al., "X-nuclei NMR self-diffusion studies in mesoporous silica foam and microporous MOF CuBTC," *Materials (Basel)*, vol. 5, no. 4, pp. 617–633, Apr. 2012. DOI: 10.3390/ma5040617.

983 984 985 986 987 [12] T. Splith, et al., "Molecular dynamics phenomena of water in the metalorganic framework MIL-100(Al), as revealed by pulsed field gradient NMR and atomistic simulation," *J. Phys. Chem. C*, vol. 121, no. 33, pp. 18065–18074, Aug. 2017. DOI: 10.1021/acs.jpcc.7b06240.

988 989 990 991 [13] C. Chmelik, et al., "Adsorption and diffusion of alkanes in CuBTC crystals investigated using infra-red microscopy and molecular simulations," *Micropor. Mesopor. Mater.*, vol. 117, no. 1–2, pp. 22–32, Jan. 2009. DOI: 10.1016/j.micromeso.2008.06.003.

992 993 994 995 [14] D. Inokuchi, et al., "Dynamics of water molecules in a 3-fold interpenetrated hydrogen-bonded organic framework based on tetrakis(4-pyridyl)methane)," *J. Phys. Chem. C*, vol. 123, no. 11, pp. 6599–6606, Feb. 2019. DOI: 10.1021/acs.jpcc.8b12421.

996 997 998 999 1000 1001 [15] M. I. Velasco, R. H. Acosta, W. A. Marmisollé, O. Azzaroni, and M. Rafti, "Modulation of hydrophilic/hydrophobic character of porous environments in metal−organic frameworks via direct polymer capping probed by NMR diffusion measurements," *J. Phys. Chem. C*, vol. 123, no. 34, pp. 21076–21082, Aug 2019. DOI: 10.1021/acs.jpcc.9b06824.

1002 1003 1004 1005 [16] J. M. Bermúdez-García, et al., "Liquid self-diffusion of H$_2$O and DMF molecules in Co-MOF-74: molecular dynamics simulations and dielectric spectroscopy studies," *Phys. Chem. Chem. Phys.*, vol. 18, no. 29,

1006 1007 pp. 19605–19612, Aug. 2016. DOI: 10.1039/C6CP02477G.

1008 1009 1010 1011 1012 1013 [17] R. Thoma, J. Kärger, N. de Sousa Amadeu, S. Nießing, and C. Janiak, "Assessing guest-molecule diffusion in heterogeneous powder samples of metal-organic frameworks through pulsed-field-gradient (PFG) NMR spectroscopy," *Chemistry*, vol. 23, no. 53, pp. 13000–13005, Sept. 2017. DOI: 10.1002/chem.201702586.

1014 1015 1016 1017 1018 [18] T. Splith, D. Fröhlich, S. K. Henninger, and F. Stallmach, "Development and application of an exchange model for anisotropic water diffusion in the microporous MOF aluminum fumarate," *J. Magn. Reson.*, vol. 291, pp. 40–46, Jun. 2018. DOI: 10.1016/j.jmr.2018.04.009.

1019 1020 1021 1022 [19] J. H. Lee, S. Jeoung, Y. G. Chung, and H. R. Moon, "Elucidation of flexible metal-organic frameworks: research progresses and recent developments," *Coord. Chem. Rev.*, vol. 389, pp. 161–188, Jun. 2019. DOI: 10.1016/j.ccr.2019.03.008.

1023 1024 1025 [20] A. Schneemann, et al., "Flexible metal-organic frameworks," *Chem. Soc. Rev.*, vol. 43, no. 16, pp. 6062–6096, Aug. 2014. DOI: 10.1039/C4CS00101J.

1026 1027 1028 1029 [21] F. Millange and R. I. Walton, "MIL-53 and its isoreticular analogues: a review of the chemistry and structure of a prototypical flexible metal-organic framework," *Isr. J. Chem.*, vol. 58, no. 9–10, pp. 1019–1035, Oct. 2018. DOI: 10.1002/ijch.201800084.

1030 1031 1032 1033 [22] D. I. Kolokolov, et al., "Probing the dynamics of the porous Zr terephthalate UiO-66 framework using 2H NMR and neutron scattering," *J. Phys. Chem. C*, vol. 116, no. 22, pp. 12131–12136, May 2012. DOI: 10.1021/jp3029193.

1034 1035 1036 1037 [23] D. I. Kolokolov, et al., "Dynamics of benzene rings in MIL-53(Cr) and MIL-47(V) frameworks studied by 2H NMR spectroscopy," *Angew. Chem. Int. Ed. Engl.*, vol. 49, no. 28, pp. 4791–4794, June 2010. DOI: 10.1002/anie.201001238.

1038 1039 1040 1041 [24] J. T. Damron, et al., "The influence of chemical modification on linker rotational dynamics in metal-organic frameworks," *Angew. Chem. Int. Ed. Engl.*, vol. 57, no. 28, pp. 8678–8681, July 2018. DOI: 10.1002/anie.201805004.

1042 1043 1044 1045 1046 1047 [25] S. Devautour-Vinot, et al., "Ligand dynamics of drug-loaded microporous zirconium terephthalates-based metal − organic frameworks: impact of the nature and concentration of the guest," *J. Phys. Chem. C*, vol. 118, no. 4, pp. 1983–1989, Jan. 2014. DOI: 10.1021/jp409753d.

1048 1049 1050 1051 1052 [26] A. E. Khudozhitkov, D. I. Kolokolov, A. G. Stepanov, V. A. Bolotov, and D. N. Dybtsev, "Metal-cation-independent dynamics of phenylene ring in microporous MOFs: a 2H solid-state NMR study," *J. Phys. Chem. C*, vol. 119, no. 50, pp. 28038–28045, Nov. 2015. DOI: 10.1021/acs.jpcc.5b09435.

1053 1054 1055 1056 [27] D. I. Kolokolov, A. G. Stepanov, and H. Jobic, "Mobility of the 2-methylimidazolate linkers in ZIF-8 probed by 2H NMR: saloon doors for the guests," *J. Phys. Chem. C*, vol. 119, no. 49, pp. 27512–27520, Nov. 2015. DOI: 10.1021/acs.jpcc.5b09312.

1057 1058 [28] S. Vaesen, et al., "A robust amino-functionalized titanium(iv) based MOF for improved separation of

acid gases," *Chem. Commun. (Camb.)*, vol. 49, no. 86, pp. 10082–10084, Nov. 2013. DOI: 10.1039/C3CC45828H.

[29] C. Zlotea, et al., "Effect of NH2 and CF3 functionalization on the hydrogen sorption properties of MOFs," *Dalton Trans.*, vol. 40, no. 18, pp. 4879–4881, May 2011. DOI: 10.1039/C1DT10115C.

[30] M. Dan-Hardi, et al., "A new photoactive crystalline highly porous titanium(IV) dicarboxylate," *J. Am. Chem. Soc.*, vol. 131, no. 31, pp. 10857–10859, Aug. 2009. DOI: 10.1021/ja903726m.

[31] F. Jeremias, V. Lozan, S. K. Henninger, and C. Janiak, "Programming MOFs for water sorption: aminofunctionalized MIL-125 and UiO-66 for heat transformation and heat storage applications," *Dalton Trans.*, vol. 42, no. 45, pp. 15967–15973, Dec. 2013. DOI: 10.1039/c3dt51471d.

[32] L. G. Gordeeva, M. V. Solovyeva, and Y. I. Aristov, "NH2-MIL-125 as a promising material for adsorptive heat transformation and storage," *Energy*, vol. 100, pp. 18–24, Apr. 2016. DOI: 10.1016/j.energy.2016.01.034.

[33] M. V. Solovyeva, Y. I. Aristov and L. G. Gordeeva, "NH2-MIL-125 as a promising adsorbent for adsorptive cooling: water adsorption dynamics," *Appl. Therm. Eng.*, vol. 116, pp. 541–548, Apr. 2017. DOI: 10.1016/j.applthermaleng.2017.01.080.

[34] P. Brandt, et al., "Metal–organic frameworks with potential application for SO_2 separation and flue gas desulfurization," *ACS Appl. Mater. Interfaces*, vol. 11, no. 19, pp. 17350–17358, May 2019. DOI: 10.1021/acsami.9b00029.

[35] P. G. Ingole, et al., "Water vapor separation from flue gas using MOF incorporated thin film nanocomposite hollow fiber membrane," *Chem. Eng. J.*, vol. 334, pp. 2450–2458, Feb. 2018. DOI: 10.1016/j.cej.2017.11.123.

[36] F. Vermoortele, et al., "p-Xylene-Selective metal-organic frameworks: a case of topology-directed selectivity," *J. Am. Chem. Soc.*, vol. 133, no. 46, pp. 18526–18529, Nov. 2011. DOI: 10.1021/ja207287h.

[37] M. A. Moreira, et al., "Adsorption equilibrium of xylene isomers and ethylbenzene on MIL-125(Ti)NH_2: The temperature influence on the para-selectivity," *Adsorption*, vol. 24, no. 8, pp. 715–724, Nov. 2018. DOI: 10.1007/s10450-018-9976-8.

[38] E. Brunner and M. Rauche, "Solid-state NMR spectroscopy: an advancing tool to analyse the structure and properties of metal-organic frameworks," *Chem. Sci.*, vol. 11, no. 17, pp. 4297–4304, May 2020. DOI: 10.1039/D0SC00735H.

[39] M. J. Barbosa Regufe, "Syngas purification using MIL-125(Ti)NH2," Master dissertation, Chemical Engineering Dept., Porto Univ, Porto, PT, 2014.

[40] D. A. Torchia, "The measurement of proton-enhanced carbon-13 T1 values by a method which suppresses artifacts," *J. Magn. Reson.*, vol. 30, no. 3, pp. 613–616, Jun. 1978. DOI: 10.1016/0022-2364(78)90288-3.

[41] D. Massiot, et al., "Modelling one- and two-dimensional solid-state NMR spectra," *Magn. Reson. Chem.*, vol. 40, no. 1, pp. 70–76, Jan. 2002. DOI: 10.1002/mrc.984.

[42] M. Geppi and C. Forte, "The SPORT-NMR software: a tool for determining relaxation times in unresolved NMR spectra," *J. Magn. Reson.*, vol. 137, no. 1, pp. 177–185, Mar. 1999. DOI: 10.1006/jmre.1998.1662.

[43] M. Mehring, *Principles of High Resolution NMR in Solids*. New York, NY: Springer, 1982.

[44] *Mathematica, Version 10.0*. Champaign, IL: Wolfram Research Inc., 2014.

[45] W. Morris, R. E. Taylor, C. Dybowski, O. M. Yaghi, and M. A. Garcia-Garibay, "Framework mobility in the metal–organic framework crystal IRMOF-3: evidence for aromatic ring and amine rotation," *J. Mol. Struct.*, vol. 1004, no. 1–3, pp. 94–101, Oct. 2011. DOI: 10.1016/j.molstruc.2011.07.037.

[46] W. P. Rothwell and J. S. Waugh, "Transverse relaxation of dipolar coupled spin systems under rf irradiation: detecting motions in solids," *J. Chem. Phys.*, vol. 74, no. 5, pp. 2721–2732, Mar. 1981. DOI: 10.1063/1.441433.

[47] S. Pizzanelli, et al., "A close view of the organic linker in a MOF: structural insights from a combined 1H NMR relaxometry and computational investigation," *Phys. Chem. Chem. Phys.*, vol. 22, no. 27, pp. 15222–15230, Jul. 2020. DOI: 10.1039/D0CP01863E.

[48] S. Hayashi, "Differential broadening between the signals split by the residual dipolar interaction with 14N in 13C CP/MAS NMR spectra of nitroanilines," *Chem. Phys. Lett.*, vol. 299, no. 3–4, pp. 272–276, Jan. 1999. DOI: 10.1016/S0009-2614(98)01284-6.

[49] N. Lock, et al., "Elucidating negative thermal expansion in MOF-5," *J. Phys. Chem. C*, vol. 114, no. 39, pp. 16181–16186, Sept. 2010. DOI: 10.1021/jp103212z.

[50] N. Lock, et al., "Scrutinizing negative thermal expansion in MOF-5 by scattering techniques and ab initio calculations," *Dalton Trans.*, vol. 42, no. 6, pp. 1996–2007, Feb. 2013. DOI: 10.1039/C2DT31491F.

[51] M. Roos, P. Micke, K. Saalwächter, and G. Hempel, "Moderate MAS enhances local 1H spin exchange and spin diffusion," *J. Magn. Reson.*, vol. 260, pp. 28–37, Nov. 2015. DOI: 10.1016/j.jmr.2015.08.016.

[52] D. E. Axelson, L. Mandelkern, R. Popli, and P. Mathieu, "Carbon-13 NMR of polyethylenes: correlation of the crystalline component T1 with structure," *J. Polym. Sci. Polym. Phys. Ed.*, vol. 21, no. 11, pp. 2319–2335, Nov. 1983. DOI: 10.1002/pol.1983.180211109.

[53] Q. Chen, et al., "Dynamic study of the noncrystalline phase of 13C-labeled polyethylene by variable-temperature 13C CP/MAS NMR spectroscopy," *J. Polym. Sci. B Polym. Phys.*, vol. 30, no. 6, pp. 591–601, May 1992. DOI: 10.1002/polb.1992.090300611.